International Journal of Control, Automation and Systems 19(1) (2021) 172-185
http://dx.doi.org/10.1007/s12555-019-0487-5
ISSN:1598-6446 eISSN:2005-4092
http://www.springer.com/12555

# Adaptive Neural Network Model-based Event-triggered Attitude Tracking Control for Spacecraft

**Hongyi Xie, Baolin Wu*, and Weixing Liu**

**Abstract:** This article investigates the problem of attitude tracking control for spacecraft with limited communication, unknown system parameters, and external disturbances. An adaptive control scheme with an event-triggered mechanism (ETM) is proposed to alleviate the communication burden. Radial Basis Function Neural Network (RBFNN) estimation model is developed to provide the input signals for the control module in this control scheme. Estimated attitude information of the spacecraft generated from the estimation model will only be transmitted to the control module at the instants when the ETM is violated. The neural network (NN) and the estimation model will be updated complying with an adaptive algorithm at the discrete triggering instants. It's substantiated that all the errors of attitude tracking converge towards corresponding residuals and there are no accumulated triggering instants. Numerical simulation also demonstrates the effectiveness of the proposed control method.

**Keywords:** Attitude tracking, event-triggered control (ETC), impulsive dynamics system, limited communication, neural networks.

## 1. INTRODUCTION

Recently, cellular satellites have received widespread attention. This conception was proposed by Tanaka in 2006 [1]. In place of a monolithic one, Tanaka divided a satellite into several standardized modules in harmony with the subsystems of the monolithic satellites, including sensor cubic-cell cellular satellites, reaction wheel cellular satellites, power cellular satellites, etc. Since all the cellular satellites are hardware-specific with shapes and structures appropriate for connecting with others, they own the priority of strong flexibility, thanks for the standardized design, even a micro spacecraft could be extended to an immense one, which is nearly impossible for a traditional monolithic spacecraft without special design. Motivated by the great potential value and the extensive prospect of application of the technology of cellular satellites, DARPA (Defense Advanced Research Projects Agency) proposed the Phoenix project [2] with a purpose to recycle the malfunctioned spacecraft. Then DLR (Deutsches Zentrum fuer Luft-und Raumfahrt e.V) proposed iBOSS (intelligent building blocks for on-orbit-satellite servicing) [3] to practice the idea of on-orbit service and extend the lifetime of their spacecraft by cellular satellites.

Inspired by the Phoenix project and actuated by the strong need of removing the space rubbish, Chang proposed that cellular satellites can take over the control of malfunctioned spacecraft [4], which is called cellular satellites attitude takeover control [5, 6]. Supposing a typical scene that an optical spacecraft with disabled attitude control system is rolling rapidly on its orbit around Earth, while with the aid of the orbit-serving robots (OSR) [7], it's probable to attach attitude control cellular satellites to the surface of this uncontrolled spacecraft [4]. Then the attitude control cellular satellites can generate control torques by themselves to stabilize the satellite, and the restored spacecraft can track a desirable attitude according to specific requirements. Since none of the known disabled spacecraft owns the standardized interfaces as the cellular satellites do, the attitude control cellular satellites connect with the disabled spacecraft without any wire or interface. Hence, both the data transmission and the energy transmission between a cellular satellite and a served spacecraft are wireless. Since cellular satellites are small modules and wireless communication is employed, the communication capability for cellular satellites is quite limited. So it's necessary to take limited communication into consideration when designing the attitude control approaches for attitude takeover control by cellular satellites.

Even if a variety of control schemes have been investigated in the field of spacecraft attitude control, for instance, adaptive control [8, 9] is used to deal with the

Manuscript received June 30, 2019; revised December 30, 2019 and March 5, 2020; accepted March 24, 2020. Recommended by Associate Editor Choon Ki Ahn under the direction of Editor Chan Gook Park. This work was supported by the National Natural Science Foundation of China under Grant 61873312

Hongyi Xie, Baolin Wu, and Weixing Liu are with the Research Center of Satellite Technology, Harbin Institute of Technology, Harbin 150001, China (e-mails: 18S118205@hit.edu.cn, wuba0001@e.ntu.edu.sg, liuweixing@hit.edu.cn).
* Corresponding author.

model uncertainty resulted from the spacecraft attitude dynamics nonlinearity, optimal control [10] and model-predictive control [11] is applied when there are some special requirements, sliding mode control [12–14] is employed to enhance the robustness of the attitude control system, iterative-learning control [15] is researched to modify the attitude control scheme online. However, all these approaches is unqualifiable to tracking the attitude of a spacecraft with limited communication without radical change. To ease the burden on the communication channel, there are two methods to deal with limited communication, quantized control [16–20] and event-triggered control [21–29], but the controlled objects of these methods are linear systems or some systems quite different from spacecraft. What's more, since spacecraft attitude tracking faces strong coupling and strong nonlinearity, it's challenging to design an attitude tracking control system with finite communication and external disturbances.

Currently, both the quantized control method and the ETM have been introduced to the field of spacecraft attitude control. The problems of attitude stabilization and attitude tracking are both investigated in [30–33] based on spacecraft attitude control with limited communication at first, but the presented method with logarithmic quantization will lead to drastic control chattering [30]. Besides, even if the approaches with hysteresis quantization in [31] could suppress the phenomenon of control chattering, spacecraft attitude control schemes with quantization are not competent for high stability attitude control mission owing to the abrupt change led by the alternation of the quantization levels. As for the method of event-triggering, Wu addressed a simple attitude stabilization control approach utilizing event-triggered mechanism [34], however, numerical simulation demonstrates that when this approach of control is applied to track the attitude of a spacecraft, it can not stabilize the attitude angular velocity error within a sufficient small bound due to the sharp variation around the triggering instants. Nevertheless, sufficient small angular velocity error is crucial for some missions, such as Time Delay Integration (TDI) imaging. There also exists an event-triggering attitude stabilization control scheme proposed by Xing *et al*. [35], although the phenomenon of control chattering is avoided in [35]. All the mentioned spacecraft attitude methods based on ETC or quantization are difficult to meet the requirement of high-stability. Because the ZOHs (zero-order holds), whose responsibility is to hold the state of a system between two consecutive triggering instants, result in sharp variation around the borders of the quantization levels or the triggering instants aperiodically.

This paper aims to provide an accurate attitude tracking control scheme with high stability for spacecraft with external disturbances and limited capability of communication. An ETM is proposed to alleviate communication pressure. An estimation model based on RBFNN and the dynamics model of spacecraft attitude tracking is proposed to displace the ZOHs, while its nonlinearity is replaced by an RBFNN term. It should be noted that the input of the controller is the state of the estimation model. Thus, except for the triggering instants when the error between the estimated attitude tracking error estimated by the estimation model and the attitude tracking error of the spacecraft violate the event-triggered condition, all the state information of the estimation model will be reset as the state of the spacecraft. It can be attested that all the states of the spacecraft and the states of the estimation model are ultimately boundedness as long as reasonable control parameters are selected. Correspondingly, simulation results demonstrate high-precision attitude tracking with high stability is realized with this model-based control scheme, control chattering is suppressed effectively and the burden of the communication channel is eased.

The remainder of this paper is structured as follows: In Section 2, the attitude tracking dynamics model of spacecraft and the main idea of NN is presented. The estimation model and the model-based control algorithm with ETM is proposed in Section 3. The ultimate bound of the dynamics system and the impossibility of Zeno behavior is validated by theoretical analysis in Section 4. The effectiveness of the proposed model-based attitude tracking control scheme is validated in Section 5. Finally, a brief conclusion could be seen in Section 6.

## 2. PROBLEM FORMULATION AND PRELIMINARIES

### 2.1. Attitude tracking dynamics

Considering the spacecraft as a rigid body and its attitude tracking dynamics can be given as follows [8]:

$$\begin{aligned}\boldsymbol{J}\dot{\boldsymbol{\omega}}_e = &-(\boldsymbol{\omega}_e + \boldsymbol{C}\boldsymbol{\omega}_d)^{\times}\boldsymbol{J}(\boldsymbol{\omega}_e + \boldsymbol{C}\boldsymbol{\omega}_d)\\ &+\boldsymbol{J}\left(\boldsymbol{\omega}_e{}^{\times}\boldsymbol{C}\boldsymbol{\omega}_d - \boldsymbol{C}\dot{\boldsymbol{\omega}}_d\right) + \boldsymbol{u} + \boldsymbol{d},\end{aligned} \tag{1}$$

$$\dot{\boldsymbol{q}}_{v,e} = \frac{1}{2}\left(\boldsymbol{q}_{v,e}^{\times} + q_{0,e}\boldsymbol{I}_3\right)\boldsymbol{\omega}_e, \tag{2}$$

$$\dot{q}_{0,e} = -\frac{1}{2}\boldsymbol{q}_{v,e}^{T}\boldsymbol{\omega}_e, \tag{3}$$

where $\boldsymbol{\omega}_d(t) \in R^3$ is the desired attitude angular velocity of the spacecraft with reference to $I$, the inertial frame. Besides, $\boldsymbol{\omega}(t) \in R^3$ denotes spacecraft's body angular with respect to $I$. $C$ denotes the rotation matrix from $I$ to the body frame of the spacecraft itself. $\boldsymbol{\omega}_e(t) = \boldsymbol{\omega}(t) - \boldsymbol{C}\boldsymbol{\omega}_d(t)$ denotes the angular velocity error of the spacecraft, in another word, the relative angular velocity of the spacecraft from its reference frame to the body frame of itself. Both $\boldsymbol{q}_{v,e}(t) \in R^3$ and $q_{0,e}(t) \in R$ are the components of the error quaternion, which shows relative orientation from the reference frame of the spacecraft to its body frame. $\boldsymbol{q}_{v,e}(t)$ is the vector component while $q_{0,e}(t)$ is the scalar component. $\boldsymbol{d}(t) \in R^3$ represents the sum of the disturbance torques from inside the spacecraft and outside it.

$\boldsymbol{I}_3$ is equal to $3 \times 3$ identity matrix, while $\boldsymbol{J} \in R^{3\times3}$ denotes the inertia matrix of the spacecraft. The notation $\boldsymbol{a}^{\times}$ denotes the skew-symmetric matrix for the vector $\boldsymbol{a} = \begin{bmatrix} a_1 & a_2 & a_3 \end{bmatrix}^T$ defined as follows:

$$\boldsymbol{a}^{\times} = \begin{bmatrix} 0 & -a_3 & a_2 \\ a_3 & 0 & -a_1 \\ -a_2 & a_1 & 0 \end{bmatrix}. \tag{4}$$

**Property 1:** The spacecraft's inertia matrix $\boldsymbol{J}$ is symmetric and positive-definite, besides, $\boldsymbol{J}$ satisfies the bounded condition as follows:

$$\boldsymbol{J}_{\min}\|x\|^2 \le \boldsymbol{x}^T\boldsymbol{J}\boldsymbol{x} \le \boldsymbol{J}_{\max}\|x\|^2, \forall \boldsymbol{J} \in R^3, \tag{5}$$

where both $\boldsymbol{J}_{\min}$ and $\boldsymbol{J}_{\max}$ are positive constants depend on the spacecraft itself. Following assumptions are useful for control law design.

**Assumption 1:** The external disturbances $\boldsymbol{d}(t)$ are hypothesized to be upper bounded with a finite positive constants, thus, $\boldsymbol{d}(t)$ satisfies $\|\boldsymbol{d}(t)\| \le \boldsymbol{d}_{\max}$, where $\boldsymbol{d}_{\max}$ is a finite positive constant [31].

**Assumption 2:** The target angular velocity of a spacecraft is bounded, that is $\|\boldsymbol{\omega}_d\| \le \omega_{d\max}$, correspondingly, its derivative $\|\dot{\boldsymbol{\omega}}_d\| \le \dot{\omega}_{d\max}$, both $\boldsymbol{\omega}_{d\max}$ and $\dot{\boldsymbol{\omega}}_{d\max}$ are confined positive constants.

## 2.2. Neural network system

The core problem of spacecraft attitude tracking is to deal with the unknown nonlinear terms with inertia matrix $\boldsymbol{J}$. In this paper, the complex dynamics nonlinear terms which include the matrix $\boldsymbol{J}$ could be estimated by NN (neural network) on a stated compact set $\Omega \subset R^3$ as

$$f(\boldsymbol{X}) = \boldsymbol{W}^T\boldsymbol{G}(\boldsymbol{X}) + \Delta\boldsymbol{X}, \tag{6}$$

where $\boldsymbol{W} \in R^l$ is the ideal weight matrix of NN to be adaptive estimated, $l > 1$ denotes the number of NN codes, $\boldsymbol{G}(\boldsymbol{X}) \in R^l$ denotes the basis function vector, besides, $\Delta\boldsymbol{X}$ is residual error, which could be restricted with $\|\Delta\boldsymbol{X}\| \le \varepsilon$ arbitrarily. Since there is an assumption that the RBFNN weight matrix $W$ is unknown, it couldn't be used for controller design directly. Thus, a novel NN based estimation scheme is applied to estimate these nonlinearities, the definition of $f(\hat{\boldsymbol{X}})$ is

$$f(\hat{\boldsymbol{X}}) = \hat{\boldsymbol{W}}^T\boldsymbol{G}(\hat{\boldsymbol{X}}), \tag{7}$$

where $\hat{\boldsymbol{W}}$ denotes the estimated matrix corresponding to the ideal RBFNN weight matrix $\boldsymbol{W}$, which is updated according to an online adaptive scheme, and $\tilde{\boldsymbol{W}} = \boldsymbol{W} - \hat{\boldsymbol{W}}$ represents the approximation error of the NN weight. Theoretically, a neural network with a reasonable number of neurons could approach all kinds of nonlinear functions [37]. Normally, the corresponding basis function could be chosen as Gaussians, sigmoid, hyperbolic tangents and so on [38–40]. While the continuous Gaussian function is chosen as the basis function $\boldsymbol{G}(\boldsymbol{X})$ [41] in this paper, which satisfies the local Lipschitz condition. Since there are n NN hidden-layer nodes, the Gaussian function follows $\boldsymbol{G}(\boldsymbol{X}) = [G_1(\boldsymbol{X}), \ldots, G_n(\boldsymbol{X})]$, while the $j_{th}$ component of the Gaussian function could be defined as follows:

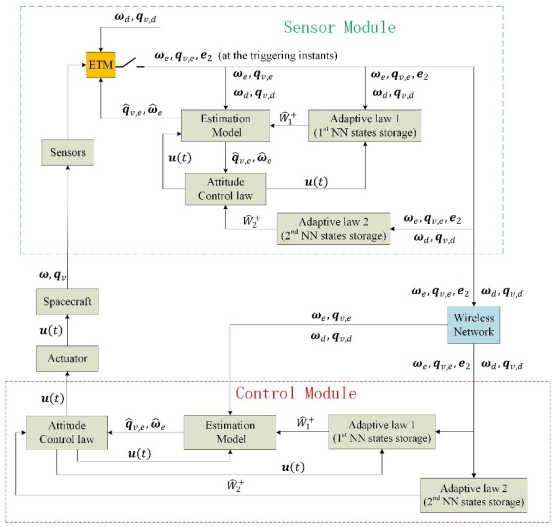


Fig. 1. Structure of the model-based spacecraft attitude tracking ETC system.

$$G_j(X) = \exp\left(\frac{-\sum_{i=1}^{m}\|\boldsymbol{X}_i - \mu_j\|^2}{H^2}\right), \quad j = 1, \ldots, n, \tag{8}$$

where $\mu_j$ represents the center of the receptive field and $H$ represents the width of the Gaussian function, $m$ denotes the quantities of input vectors. Since more than one state vectors are estimated by a RBFNN, $\boldsymbol{X}$ and $\hat{\boldsymbol{X}}$ are matrixes which consist of multiple vectors, $X_i$ represents the $i_{th}$ vector element of $\boldsymbol{X} = \{\boldsymbol{X}_1, \ldots, \boldsymbol{X}_i, \ldots, \boldsymbol{X}_m\}$, while $\hat{\boldsymbol{X}}_i$ denotes the $i_{th}$ component of $\hat{\boldsymbol{X}} = \left\{\hat{\boldsymbol{X}}_1, \hat{\boldsymbol{X}}_2, \ldots, \hat{\boldsymbol{X}}_i, \ldots, \hat{\boldsymbol{X}}_m\right\}$ homogenously.

**Assumption 3** [27]**:** The desired NN weight matrix $\boldsymbol{W}$ and the corresponding activation function $\boldsymbol{G}$ are upper bounded, which follow $\|\boldsymbol{W}\| \le W_M$ and $\|\boldsymbol{G}(\boldsymbol{X})\| \le G_M$, where $W_M$ and $G_M$ are finite positive constants.

**Assumption 4** [27]**:** The activated function $\boldsymbol{G}$ meets the locally Lipschitz continuity condition, which follows $\|\boldsymbol{G}(\boldsymbol{X}) - \boldsymbol{G}(\hat{\boldsymbol{X}})\| \le l\left\|\sum_{i=1}^{m}(\boldsymbol{X}_i - \hat{\boldsymbol{X}}_i)\right\|$.

**Remark 1:** There are two NN used in this paper, the first NN is applied to estimate the dynamics expression of $\hat{\boldsymbol{s}}$ in the estimation model and the second NN is applied to estimate the nonlinear term $\boldsymbol{L}$. For simplicity, the subscripts of them will be omitted when it's not necessary.

### 2.3. Problem formulation

The purpose of this paper is to put forward a model-based attitude tracking control law with the aid of ETM to decrease the quantities of data to be sent over the channel of communication. Besides, to ensure that all the signals transmitted in this ETC system are ultimately bounded.

The proposed neural network model-based attitude tracking ETC system over the communication channel with limited communication is demonstrated in Fig. 1. The signals of control torque are sent from the controller to both the spacecraft actuators and the estimation model over the wireless network. Different from normal event-triggered mechanisms that compare the state of a system with its state at the last triggering instants, an estimation model is introduced instead of the ZOHs (zero-order holds) in this paper. The estimated attitude tracking errors $\widehat{\boldsymbol{\omega}}_e, \widehat{\boldsymbol{q}}_{v,e}$ will be computed and memorized by the module of estimation model itself, and the difference between $\widehat{\boldsymbol{\omega}}_e$ and $\boldsymbol{\omega}_e$ will be calculated just before the triggering instants, which is defined as $\boldsymbol{e}_2$ in (20). Once the error between the spacecraft dynamics model and the estimation model violate the event-trigger condition, all the states estimated by the estimation model will be reset as the attitude information measured by the sensors at triggering instants, $\widehat{\boldsymbol{q}}_{v,e}^{+} = \boldsymbol{q}_{v,e}$, $\widehat{\boldsymbol{\omega}}_e^{+} = \boldsymbol{\omega}_e$, will be applied to renew the state of the estimation model, while $\boldsymbol{e}_2 = \boldsymbol{\omega}_e - \widehat{\boldsymbol{\omega}}_e$ will be transmitted to update the adaptive law. Besides, the discrete state of NN weight matrix will be stored in the adaptive law module, once a novel $\boldsymbol{e}_2$ is transmitted to the adaptive law module at triggering instants, a new NN weight matrix will be gained owing to the adaptive law, which is an essential part of the estimation model and control law. Except for all the above mentioned, the attitude control module receives the estimated attitude information from the estimation model, and the attitude control module generates corresponding control torque, which will be feedback to the estimation model, form a simple closed loop.

### 2.4. The production of control torques

In this paper, although the control module can acquire new inputs from the sensor module only at the triggering instants. However, according to the structure of the control system demonstrated in Fig. 1 in our manuscript, when it is during the flow states (not at the triggering instants, defined in section 3), the estimation model in the control module will transmit its estimated states to the controller, and the controller will generate consecutive control signals. Meanwhile, the states of the estimation model will also vary with the consecutive control signals, so the controller and the estimation model form a virtue consecutive closed-loop control system. Therefore, the controller can generate consecutive control signals according to the state variation of the estimation model during the flow period, then those consecutive control signals will be transmitted to the actuators and the attitude parameters of the spacecraft will vary smoothly with the consecutive smooth control signals [27]. Thus, the response of the system states is consecutive and smooth during the flow period.

While at the triggering instants, the errors between the state parameters measured by the sensors and the estimated state parameters calculated by the estimation module inside the sensor module violate the event-triggered mechanism, there exists the risk of worse precision of attitude tracking. Thus, at the triggering instants, the event-triggered mechanism is triggered, and the state parameters measured by the sensor at the triggering instants will be sent to the controller over the wireless communication channel instantly [26, 27]. Once the new signals arrive at the controller module, the states of the estimation module will be updated and the controller will generate new control signals with the variation of the estimation model in the following flow period. Thus, the control precision can be permitted by the timely update of the estimation model and the consecutive control torques generated from the estimation model during the flow period.

Although the control law changed suddenly at the triggering instants, however, the sudden alteration of the control law only influences the variation rate of the system states, the smoothness of the system states will not be influenced as a result of the jump of the control law [27].

## 3. MODEL-BASED ADAPTIVE EVENT-TRIGGERED CONTROLLER DESIGN

In this section, a model-based adaptive controller with ETM and a corresponding estimation model is proposed for the spacecraft attitude tracking dynamics system described in (1)-(3) with the existence of all kinds of disturbances (gravity gradient moment, solar pressure moment, aerodynamic moment, magnetic moment [36] and unknown internal disturbance) to relieve the pressure over the wireless communication channel. To develop the estimation model, the sliding vector is given as follows:

$$\boldsymbol{s} = k_1 \boldsymbol{q}_{v,e} + \boldsymbol{\omega}_e, \tag{9}$$

where $k_1 \in (0,1)$, similarly, the estimated sliding vector is proposed as follows:

$$\widehat{\boldsymbol{s}} = \widehat{\boldsymbol{\omega}}_e + k_1 \widehat{\boldsymbol{q}}_{v,e}, \tag{10}$$

where $\hat{\boldsymbol{s}}$, $\widehat{\boldsymbol{\omega}}_e$, $\widehat{\boldsymbol{q}}_{v,e}$ are the estimation of $\boldsymbol{s}$, $\boldsymbol{\omega}_e$, $\boldsymbol{q}_{v,e}$. The key to establishing an estimation model is to estimate the nonlinearities of attitude tracking, while the nonlinear term of the spacecraft dynamics model could be extracted from dynamic function (1)

$$\begin{aligned}\boldsymbol{L} = &-(\boldsymbol{\omega}_e + \boldsymbol{C}\boldsymbol{\omega}_d)^{\times}\boldsymbol{J}(\boldsymbol{\omega}_e + \boldsymbol{C}\boldsymbol{\omega}_d) + \boldsymbol{J}\boldsymbol{\omega}_e^{\times}\boldsymbol{C}\boldsymbol{\omega}_d \\ &- \boldsymbol{J}\boldsymbol{C}\dot{\boldsymbol{\omega}}_d + \frac{k_1}{2}\boldsymbol{J}\left(\boldsymbol{q}_{v,e}^{\times} + q_{0e}\boldsymbol{I}_3\right)\boldsymbol{\omega}_e.\end{aligned} \tag{11}$$

According to (11), it's reasonable to acquire another form of the attitude tracking dynamic function

$$\boldsymbol{J}\dot{\boldsymbol{s}} = \boldsymbol{L} + \boldsymbol{u} + \boldsymbol{d}. \tag{12}$$

While (12) could be rewritten as

$$\dot{\boldsymbol{s}} = \boldsymbol{J}^{-1}(\boldsymbol{L} + \boldsymbol{u} + \boldsymbol{d}) = \boldsymbol{J}^{-1}(\boldsymbol{L} + \boldsymbol{u}) + \boldsymbol{J}^{-1}\boldsymbol{d}. \tag{13}$$

From (6), (13) could be rewritten as following form

$$\dot{\boldsymbol{s}} = \boldsymbol{W}_1^T \boldsymbol{G}(\boldsymbol{X}_1) + \Delta \boldsymbol{X}_1, \tag{14}$$

where $\boldsymbol{X}_1 = \{\boldsymbol{\omega}_e, \boldsymbol{\omega}_d, k_1 \boldsymbol{q}_{v,e}, \dot{\boldsymbol{\omega}}_d, \boldsymbol{u}\}$, $\boldsymbol{W}_1^T \boldsymbol{G}(\boldsymbol{X}_1)$ is the estimation of $\boldsymbol{J}^{-1}(\boldsymbol{L} + \boldsymbol{u}) + \boldsymbol{J}^{-1}\boldsymbol{d}$, and $\Delta \boldsymbol{X}_1$ is the corresponding residual error of this estimation. According to Fig. 1, since the estimation model could not acquire any $\omega_e$ or $\boldsymbol{q}_{v,e}$ during the stages of flow, it's reasonable to replace $\boldsymbol{W}_1^T \boldsymbol{G}(\boldsymbol{X}_1)$ by $\widehat{\boldsymbol{W}}_1^T \boldsymbol{G}\left(\hat{\boldsymbol{X}}_1\right)$ in the estimation model, the corresponding estimated sliding vector inside the estimation model could be given as follows:

$$\dot{\hat{\boldsymbol{s}}} = \widehat{\boldsymbol{W}}_1^T \boldsymbol{G}\left(\hat{\boldsymbol{X}}_1\right), \tag{15}$$

where $\hat{\boldsymbol{X}}_1 = \left\{\widehat{\boldsymbol{\omega}}_e, \boldsymbol{\omega}_d, k_1 \widehat{\boldsymbol{q}}_{v,e}, \dot{\boldsymbol{\omega}}_d, \boldsymbol{u}\right\}$, $\boldsymbol{u}$ represents the control torque. Since (15) is the estimation form which is derived from (1), (2) could be rewritten as $\dot{\widehat{\boldsymbol{q}}}_{v,e} = \frac{1}{2}\left(\widehat{\boldsymbol{q}}_{v,e}^{\times} + \hat{q}_{0,e}\boldsymbol{I}_3\right)\widehat{\boldsymbol{\omega}}_e$ while (3) could be rewritten as $\dot{\hat{q}}_{0,e} = -\frac{1}{2}\widehat{\boldsymbol{q}}_{v,e}^T \widehat{\boldsymbol{\omega}}_e$, thus, the dynamic equations within the estimation model is concluded as follows:

$$\begin{cases} \dot{\hat{\boldsymbol{s}}} = \widehat{\boldsymbol{W}}_1^T \boldsymbol{G}\left(\hat{X}_1\right), \ \ \dot{\hat{q}}_{0,e} = -\frac{1}{2}\widehat{\boldsymbol{q}}_{v,e}^T \widehat{\boldsymbol{\omega}}_e, \\ \dot{\widehat{\boldsymbol{q}}}_{v,e} = \frac{1}{2}\left(\widehat{\boldsymbol{q}}_{v,e}^{\times} + \hat{q}_{0,e}\boldsymbol{I}_3\right)\widehat{\boldsymbol{\omega}}_e. \end{cases} \tag{16}$$

Since $\dot{\hat{\boldsymbol{s}}} = \widehat{\boldsymbol{W}}_1^T \boldsymbol{G}\left(\hat{\boldsymbol{X}}_1\right)$ could represent (1) in the estimation model (16), it's appropriate to rewritten the nonlinear term (11) as the following one:

$$\boldsymbol{L} = \boldsymbol{W}_2^T \boldsymbol{G}(\boldsymbol{X}_2) + \Delta \boldsymbol{X}_2, \tag{17}$$

where $\boldsymbol{G}(\boldsymbol{X}_2) = \boldsymbol{G}(\boldsymbol{\omega}_e, \boldsymbol{\omega}_d, k_1 \boldsymbol{q}_{v,e}, \dot{\boldsymbol{\omega}}_d)$ and the estimated form of (17), also a component of $\boldsymbol{u}$, could be written as

$$\hat{\boldsymbol{L}} = \widehat{\boldsymbol{W}}_2^T \boldsymbol{G}\left(\hat{\boldsymbol{X}}_2\right) = \widehat{\boldsymbol{W}}_2^T \boldsymbol{G}\left(\widehat{\boldsymbol{\omega}}_e, \boldsymbol{\omega}_d, k_1 \widehat{q}_{v,e}, \dot{\boldsymbol{\omega}}_d\right). \tag{18}$$

From the estimation nonlinear term (18), the control law could be proposed as follows [27]:

$$\boldsymbol{u}(t) = -k_2 \hat{\boldsymbol{s}} - \hat{\boldsymbol{L}} = -k_2 \hat{\boldsymbol{s}} - \widehat{\boldsymbol{W}}_2^T \boldsymbol{G}\left(\hat{\boldsymbol{X}}_2\right), \tag{19}$$

where $k_2$ is a positive constant. Since $\boldsymbol{u}(t)$ is one of the inputs of the estimation model (15), it's reasonable to consider the initial instant of the process of spacecraft attitude tracking control as an event-triggering instant so that the state signals of the spacecraft could be transmitted to the estimation model, therefore, the proposed could start its working. Consequently, considering the difference between the state of the spacecraft and the state estimated by the estimation model as the event-triggering error, the definition of the event-trigger error, $e_1, e_2$ could be given as follows:

$$\boldsymbol{e} = \boldsymbol{s} - \hat{\boldsymbol{s}}, \ \ \boldsymbol{e}_1 = \boldsymbol{q}_{v,e} - \widehat{\boldsymbol{q}}_{v,e} = \widetilde{\boldsymbol{q}}_{v,e}, \ \ \boldsymbol{e}_2 = \boldsymbol{\omega}_e - \widehat{\boldsymbol{\omega}}_e = \widetilde{\boldsymbol{\omega}}_e. \tag{20}$$

Then it's reasonable to take following event trigger condition into consideration:

$$\|\boldsymbol{e}\| < \alpha \|\boldsymbol{s}\| + \gamma, \tag{21}$$

where $\alpha \in (0,1)$, $\gamma$ denotes a very small parameter which is employed to avoid ZENO behavior. When the condition of ETM is violated, all the states estimated by the estimation model will be updated at these event sampling instants, which meet

$$\widehat{\boldsymbol{q}}_{v,e}^{+} = \boldsymbol{q}_{v,e}, \ \ \widehat{\boldsymbol{\omega}}_e^{+} = \boldsymbol{\omega}_e, \ \ t = t_k. \tag{22}$$

NN weight matrices $\widehat{\boldsymbol{W}}_1, \widehat{\boldsymbol{W}}_2$ are constants during the flow state, while to keep pace with the attitude variation of the spacecraft, an adaptive law for NN weight matrix update is proposed. Here give out two novel concepts of flow state and jump state. The flow state denotes the system state between two contiguous triggering instants, while the jump state denotes the system state at the instants of triggering. $\widehat{\boldsymbol{W}}_1, \widehat{\boldsymbol{W}}_2$ keep invariable during the flow state, only at the instants the condition of ETM is violated (jump state) will the NN weight matrix be updated. Hence, compared with previous spacecraft control scheme based on the concept of NN, the amount of calculation could be reduced drastically owing to the proposed control scheme, meanwhile, the burden of the communication channel could be relaxed significantly.

Correspondingly, the update law of NN weight matrixes at the event-triggering instants, also the adaptive law could be defined as the following form, since this proposed adaptive update algorithm is suitable for both $\widehat{\boldsymbol{W}}_1$ and $\widehat{\boldsymbol{W}}_2$, for simplicity, the subscripts of $\widehat{\boldsymbol{W}}$, $\sigma$, $\beta$, $c$ and $\hat{\boldsymbol{X}}$ have been omitted according to Remark 1.

$$\widehat{\boldsymbol{W}}^{+} = (1 - \sigma)\widehat{\boldsymbol{W}} - \beta \frac{\boldsymbol{e}_2(t)}{c + \|\boldsymbol{e}_2^T(t)\boldsymbol{e}_2(t)\|} \boldsymbol{G}(\hat{\boldsymbol{X}}), \tag{23}$$

where $\widehat{\boldsymbol{W}}^{+}$ denotes the estimation of the updated RBFNN weight matrix just after the jump state. $\sigma$ is the adaptive parameter, which is a positive constant. $\beta$ represents the learning rate of the NN, besides, $c$ is a positive constant. Notice that $\widehat{\boldsymbol{q}}_{v,e} = \boldsymbol{q}_{v,e}$, $\widehat{\boldsymbol{\omega}}_e = \boldsymbol{\omega}_e$ at the event-triggering instant, the input of RBF (Radial Basis Function) $\boldsymbol{G}$ is the state of the spacecraft at the instant of event-triggering, also the state of the estimation model. Besides, the NN weight matrix comply with following update law during the flow state:

$$\dot{\widehat{\boldsymbol{W}}} = 0 \text{ when } t_k < t \le t_{k+1}. \tag{24}$$

According to (23) with $\widetilde{\boldsymbol{W}} = \boldsymbol{W} - \widehat{\boldsymbol{W}}$, it's easy to achieve the update rule of $\widetilde{\boldsymbol{W}}$ at the jump instants

$$\begin{aligned}\widetilde{\boldsymbol{W}}^{+} &= \boldsymbol{W} - \widehat{\boldsymbol{W}}^{+} = \sigma\widehat{\boldsymbol{W}} + \widetilde{\boldsymbol{W}} + \beta\lambda\boldsymbol{G} \\ &= \sigma\widehat{\boldsymbol{W}} + \widetilde{\boldsymbol{W}} + \beta\frac{\boldsymbol{e}_2(t)}{c + \|\boldsymbol{e}_2^T(t)\boldsymbol{e}_2(t)\|}\boldsymbol{G}(\boldsymbol{X}).\end{aligned} \tag{25}$$

And the variation law of $\widetilde{\boldsymbol{W}}$ during the flow period

$$\dot{\widetilde{\boldsymbol{W}}} = 0, \text{ when } t_k < t \le t_{k+1}. \tag{26}$$

Compared with traditional NN based control methods applied in spacecraft attitude tracking, in this paper, the NN weights are not reset periodically. Hence, the load of transmission could be obviously alleviated.

**Remark 2:** Except for spacecraft attitude take over control, this model-based control scheme can play its role in all kinds of spacecraft with the problem of limited communication in their control system, including low-cost micro spacecraft and plug-and-play spacecraft.

**Remark 3:** The control parameter $k_1$ in (9) and the control gain $k_1$ in (19) are chosen as [31] $k_1k_2 = 2\omega_n^2\|\boldsymbol{J}\|, k_2 = 2\xi\omega_n\|\boldsymbol{J}\|, \omega_n = 8/t_s$, where $\xi$ denotes the damping ratio, $\omega_n$ denotes the natural frequency, $t_s$ denotes the setting time decided by system mission.

## 4. STABILITY ANALYSIS AND ZENO BEHAVIOR ANALYSIS

In this section, the analysis of control stability and the boundedness verification of all the signals in this spacecraft attitude tracking control system will be presented, Generally, this section could be divided into three steps. First, the boundedness of the estimation errors of the NN weight would be presented based on that in [27]. Second, the boundedness of the system states could be proved by the Lyapunov approach. Finally, the existence of the minimum IET(inter-execution time) will be given to demonstrate that there will be no Zeno behavior in the process of controlling.

In consideration of the complex dynamic performance of the spacecraft with event-triggering mechanism, each step of the stability analysis with this control scheme will be divided into two parts in the remainder of this paper: flow state and jump instants. Flow state denotes the state that the closed-loop model is flowing and the event-triggered condition is not infringed, while the jump instants denote the instants when the condition of ETM is infringed and the system is reset.

### 4.1. The ultimate boundedness of the NN weight estimation errors

Theorem 1 below demonstrates the locally ultimate boundedness of the estimation errors of the RBFNN weights $\widetilde{\boldsymbol{W}}_1, \widetilde{\boldsymbol{W}}_2$.

**Theorem 1:** Given the estimation model (15), the control algorithm (19) with the adaptive renew law of RBFNN weight matrixes (25) and (26) under Assumption 3, the errors of the RBFNN weight matrixes $\widetilde{\boldsymbol{W}}_1$, $\widetilde{\boldsymbol{W}}_2$ are locally ultimately bounded for all the instants of event- triggering.

**Proof:** The verification of the upper boundedness of the RBFNN weight matrixes approximation errors is carried out with two different part: flow period and jump instants.

**Circumstance 1 Flow period** ($t_k < t \le t_{k+1}$, $k = 1, 2, \ldots$)**:** Select the candidate of Lyapunov function as follows:

$$V_{\widetilde{W}} = \mathrm{tr}\left(\widetilde{\boldsymbol{W}}_1^T\widetilde{\boldsymbol{W}}_1\right) + \mathrm{tr}\left(\widetilde{\boldsymbol{W}}_2^T\widetilde{\boldsymbol{W}}_2\right) = const. \tag{27}$$

And the derivative of (27) with respect to time satisfies

$$\dot{V}_{\widetilde{W}} = \mathrm{tr}\left(\widetilde{\boldsymbol{W}}_1^T\dot{\widetilde{\boldsymbol{W}}}_1\right) + \mathrm{tr}\left(\widetilde{\boldsymbol{W}}_2^T\dot{\widetilde{\boldsymbol{W}}}_2\right) = 0 \tag{28}$$

where $\mathrm{tr}\,(A_{n\times n}) = \sum_{i=1}^{n} a_{ii}$, from(28), the first derivative $\dot{V}_{\widetilde{W}} = 0$ proves that the estimation errors of the RBFNN weight remain constant during the period of flowing. Considering that one of the initial NN weight matrixes follows $\widehat{\boldsymbol{W}}(0) = 0$, and the ideal weight matrix of NN $\boldsymbol{W}$ is upper bounded with (39), the initial approximation errors of the NN weights must be bounded. Thus, the boundedness of $\widetilde{\boldsymbol{W}}$ under all circumstances will be proved as long as the boundedness of $\widetilde{\boldsymbol{W}}$ is proved at the instants of jumping.

**Circumstance 2 Jump instants** ($t = t_k$, $k = 1, 2, \ldots$)**:** Transform (28) into a discrete form. It could be proved that the first difference of this discrete candidate of Lyapunov function is locally ultimately bounded during the jump instants. According to Remark 1, since $\widetilde{\boldsymbol{W}}_1$ and $\widetilde{\boldsymbol{W}}_2$ present identical properties during the process of stability analysis, a single $\widetilde{\boldsymbol{W}}$ could represent $\widetilde{\boldsymbol{W}}_1$ and $\widetilde{\boldsymbol{W}}_2$ in this part of stability analysis, thus, the discrete candidate of Lyapunov function could be proposed as follows:

$$\Delta V_{\widetilde{W}} = \mathrm{tr}\left(\widetilde{\boldsymbol{W}}^{T+}\widetilde{\boldsymbol{W}}^{+}\right) - \mathrm{tr}\left(\widetilde{\boldsymbol{W}}^T\widetilde{\boldsymbol{W}}\right). \tag{29}$$

Consider $\widehat{\boldsymbol{W}} = \boldsymbol{W} - \widetilde{\boldsymbol{W}}$, substitute (23) into (29) leads to

$$\begin{aligned}\Delta V_{\widetilde{W}} =& \mathrm{tr}(\widetilde{\boldsymbol{W}} + \beta\lambda G + \sigma\widehat{\boldsymbol{W}})^T \times (\widetilde{\boldsymbol{W}} + \beta\lambda G + \sigma\widehat{\boldsymbol{W}}) \\ &- \mathrm{tr}\left(\widetilde{\boldsymbol{W}}^T\widetilde{\boldsymbol{W}}\right) = 2\beta\lambda\,\mathrm{tr}\left(\widetilde{\boldsymbol{W}}^T G\right) + 2\sigma\,\mathrm{tr}\left(\widetilde{\boldsymbol{W}}^T\hat{\boldsymbol{W}}\right) \\ &- 2\sigma\,\mathrm{tr}\left(\widetilde{\boldsymbol{W}}^T\hat{\boldsymbol{W}}\right) + \beta^2\lambda^2\,\mathrm{tr}\left(G^T G\right) \\ &+ 2\beta\sigma\lambda\,\mathrm{tr}\left(G^T\widehat{\boldsymbol{W}}\right) - 2\beta\sigma\lambda\,\mathrm{tr}\left(G^T\widehat{\boldsymbol{W}}\right) \\ &+ \sigma^2\,\mathrm{tr}\left((\boldsymbol{W} - \widetilde{\boldsymbol{W}})^T(\boldsymbol{W} - \widetilde{\boldsymbol{W}})\right).\end{aligned} \tag{30}$$

In virtue of average inequality $2\|\boldsymbol{W}\|\|\widetilde{\boldsymbol{W}}\| \le \|\widetilde{\boldsymbol{W}}\|^2 + \|\boldsymbol{W}\|^2$, (30) could be rewritten as follows:

$$\Delta V_{\widetilde{W}} \le 2\beta\lambda G_M(1-\sigma)\|\widetilde{\boldsymbol{W}}\| + \beta^2\lambda^2 G_M^2$$

$$+2\sigma^2\|\boldsymbol{W}\|^2+2\sigma\|\boldsymbol{W}\|\|\widetilde{\boldsymbol{W}}\| -2\sigma(1-\sigma)\|\widetilde{\boldsymbol{W}}\|^2+2\beta\sigma\lambda G_M\|\boldsymbol{W}\|. \quad (31)$$

Define

$$\zeta=2\beta\sigma\lambda G_M W_M+2\sigma^2W_M^2+\beta^2\lambda^2G_M^2. \quad (32)$$

Substituting (32) into (31) yields

$$\Delta V_{\widetilde{W}} \le 2\beta\lambda G_M(1-\sigma)\|\widetilde{\boldsymbol{W}}\|+\zeta +2\sigma W_M\|\widetilde{\boldsymbol{W}}\|-2\sigma(1-\sigma)\|\widetilde{\boldsymbol{W}}\|^2. \quad (33)$$

Define $p_1$, $p_2$ as follows:

$$p_1=2\sigma(1-\sigma)>0, p_2=2\beta\lambda G_M(1-\sigma)+2\sigma W_M, \quad (34)$$

where $0<\sigma<0.5$. In view of(34), (33) could be rewritten as

$$\Delta V_{\widetilde{W}} \le -p_1\|\widetilde{\boldsymbol{W}}\|^2+p_2\|\widetilde{\boldsymbol{W}}\|+\zeta. \quad (35)$$

Define

$$\overline{\zeta}=\zeta+p_2^2/2p_1. \quad (36)$$

Substituting (36) into (35) yields

$$\Delta V_{\widetilde{W}} \le -\frac{1}{2}p_1\|\widetilde{\boldsymbol{W}}\|^2-\frac{1}{2}p_1\left(\|\widetilde{\boldsymbol{W}}\|-\frac{p_2}{p_1}\right)^2+\overline{\zeta}. \quad (37)$$

Note that $-\frac{1}{2}p_1\left(\|\widetilde{\boldsymbol{W}}\|-\frac{p_2}{p_1}\right)^2\le 0$, the first difference $\Delta V_{\widetilde{W}}<0$, as long as

$$\|\widetilde{\boldsymbol{W}}\|\ge\sqrt{2\overline{\zeta}/p_1}. \quad (38)$$

Therefore, the estimation errors of the RBFNN weight matrices are ultimately bounded at the jump instants, which follows

$$\|\tilde{\boldsymbol{W}}\|\le\left[\frac{2W_M(\beta G_M+\sigma W_M)}{1-\sigma}+\frac{\beta^2\lambda^2G_M^2}{\sigma^2(1-\sigma)} +\left(\frac{W_m}{1-\sigma}\right)^2\right]^{1/2}, \quad (39)$$

where $\sigma$, $\beta$, $\lambda$, $G_M$, $W_M$ are all constants, thus, it could be concluded from (27), (28), (29), (39) that the estimation error of the NN weight matrix is ultimately bounded with an upper bound given by (39). Since $W_1$ and $W_2$ are upper bounded with $W_{1,M}$ and $W_{2,M}$, and the local boundedness of $\widetilde{\boldsymbol{W}}_1$ and $\widetilde{\boldsymbol{W}}_2$ are verified, $\widehat{\boldsymbol{W}}_1$ and $\widehat{\boldsymbol{W}}_2$ are locally ultimately bounded with their upper bound $\widehat{W}_{1M}$ and $\widehat{W}_{2M}$. □

### 4.2. Boundedness of all the system states

In this section, the stability analysis and the boundedness verification of the impulsive dynamics system will be shown. Since the local boundedness of $\boldsymbol{W}_1$, $\boldsymbol{W}_2$, $\widehat{\boldsymbol{W}}_1$, $\widehat{\boldsymbol{W}}_2$ have been guaranteed, as long as $\boldsymbol{G}\left(\hat{\boldsymbol{X}}_2\right)$ is ultimately bounded, the difference $\widetilde{\boldsymbol{L}}$ between the estimated nonlinear term $\boldsymbol{L}$ will be finite. However, in order to verify the ultimate boundedness of $\widetilde{\boldsymbol{L}}$, it is inevitable to take advantage of Assumption 4, that's to say, it is unavoidable to prove the ultimate boundedness of $\boldsymbol{e}_1=\boldsymbol{q}_{v,e}-\widehat{\boldsymbol{q}}_{v,e}$ and $\boldsymbol{e}_2=\boldsymbol{\omega}_e-\widehat{\boldsymbol{\omega}}_e$. Thanks for the work of Boskovic [12] which verified that $\boldsymbol{q}_{v,e}$ and $\boldsymbol{\omega}_e$ will converge to zero as $t\to\infty$ on $\boldsymbol{s}=0$, it's reasonable to deduce that the ultimate boundedness of $\boldsymbol{s}$ signifies the ultimate boundedness of $\boldsymbol{q}_{v,e}$ and $\boldsymbol{\omega}_e$, similarly, the ultimate boundedness of $\hat{\boldsymbol{s}}$ signifies the ultimate boundedness of $\widehat{\boldsymbol{q}}_{v,e}$ and $\widehat{\boldsymbol{\omega}}_e$. Thus, several theorems will be proposed to ensure the ultimate boundedness of all these variables when the ultimate boundedness of the sliding vector $\boldsymbol{s}$ and $\hat{\boldsymbol{s}}$ is guaranteed. In view of Assumption 3, Assumption 4 and Theorem 1, the ultimate bound of $\tilde{\boldsymbol{L}}$ can be concluded as

$$\begin{aligned}\|\tilde{\boldsymbol{L}}\|=&\|\boldsymbol{L}-\hat{\boldsymbol{L}}\|=\left\|\boldsymbol{W}_2^T\boldsymbol{G}(\boldsymbol{X}_2)+\Delta\boldsymbol{X}_2-\widehat{\boldsymbol{W}}_2^T\boldsymbol{G}\left(\hat{\boldsymbol{X}}_2\right)\right\|\\ =&\left\|\widetilde{\boldsymbol{W}}_2^T\boldsymbol{G}(\boldsymbol{X}_2)+\widehat{\boldsymbol{W}}_2^T\left[\boldsymbol{G}(\boldsymbol{X}_2)-\boldsymbol{G}\left(\hat{\boldsymbol{X}}_2\right)\right]+\Delta X_2\right\|\\ \le&\left\|\widehat{\boldsymbol{W}}_2\right\|\left\|k_1\left(\boldsymbol{q}_{v,e}^T-\widehat{\boldsymbol{q}}_{v,e}^T\right)+\boldsymbol{\omega}_e^T-\widehat{\boldsymbol{\omega}}_e^T\right\|+\varepsilon_2\\ &+\left\|\tilde{\boldsymbol{W}}_2\right\|G_{2M}\\ \le&\left\|\tilde{\boldsymbol{W}}_2\right\|G_{2M}+\left\|\boldsymbol{W}_2-\tilde{\boldsymbol{W}}_2\right\|\|\boldsymbol{e}\|+\varepsilon_2\\ \le&\left\|\widetilde{\boldsymbol{W}}_2\right\|G_{2M}+l_2\left(W_{2M}+\left\|\widetilde{\boldsymbol{W}}_2\right\|\right)\|\boldsymbol{s}\|+\varepsilon_2, \quad (40)\end{aligned}$$

where $\alpha$, $\gamma$, $G_{2M}$, $l_2$, $W_{2M}$, $\varepsilon_2$ are positive constants, the upper boundedness of $\left\|\widetilde{\boldsymbol{W}}_2\right\|$ is verified by (39), while $\|\boldsymbol{s}\|$ is a variable. Thus, the definite upper bound of $\|\tilde{\boldsymbol{L}}\|$ is still unknown, however, (40) could play an important role in the following content of verification.

**Theorem 2:** Consider the attitude dynamics model of the spacecraft(1-3), the estimation model (15), the ultimate bound of $\widetilde{\boldsymbol{W}}_1$ and $\widetilde{\boldsymbol{W}}_2$ (39), inequation (40), and Assumptions 1 to 4. If the control law in (19) is implemented, then both the attitude tracking error of the spacecraft and the corresponding one estimated by the estimation model are ultimately bounded.

**Proof:** The analysis of control stability could be divided into two parts: Flow period and jump instants. All of the variable states, including the variables within the estimation model and the variables inside the control law, will be considered within a monolith whenever it is in flow period or jump instants.

**Circumstance 1 Flow period** ($t_k<t\le t_{k+1}$, $k=1, 2, \ldots$)**:** Select the candidate of Lyapunov function as follows:

$$V=V_f+V_{\hat{f}}+V_{\widetilde{W}_1}+V_{\widetilde{W}_2}, \quad (41)$$

where $V_f = \frac{1}{2}\boldsymbol{s}^T\boldsymbol{J}\boldsymbol{s}$, $V_{\hat{f}} = \frac{1}{2}\hat{\boldsymbol{s}}^T\hat{\boldsymbol{s}}$, and $V_{\widetilde{W}_1}$, $V_{\widetilde{W}_2}$ have been defined in Theorem 1. In view of event-trigger error (20), event-trigger condition (21) and inequation (40), the derivative of $V_f = \frac{1}{2}\boldsymbol{s}^T\boldsymbol{J}\boldsymbol{s}$ satisfies following inequation:

$$\begin{aligned}\dot{V}_f =&\boldsymbol{s}^T\boldsymbol{J}\dot{\boldsymbol{s}} = \boldsymbol{s}^T(\boldsymbol{L}+\boldsymbol{u}+\boldsymbol{d})\\ =&\boldsymbol{s}^T\left(\tilde{\boldsymbol{L}} - k_2\boldsymbol{s} + k_2\boldsymbol{e}\right)\|\boldsymbol{s}\|\,\|\boldsymbol{d}_{\max}\|\\ \le& -k_2\|\boldsymbol{s}\|^2 + k_2\|\boldsymbol{s}\|(\alpha\|\boldsymbol{s}\|+\gamma)\\ &+\|\boldsymbol{s}\|\|\tilde{\boldsymbol{L}}\| + \|\boldsymbol{s}\|\,\|\boldsymbol{d}_{\max}\|\\ \le&\left[(\alpha-1)k_2 + l_2\left(W_{2M} + \left\|\widetilde{\boldsymbol{W}}_2\right\|\right)\right]\|\boldsymbol{s}\|^2\\ &+\{\|\boldsymbol{d}_{\max}\| + \gamma k_2 + \varepsilon_2 + \gamma l_2 W_{2M}\}\|\boldsymbol{s}\|\\ &+\left\|\widetilde{\boldsymbol{W}}_2\right\|(G_{2M}+\gamma l_2)\|\boldsymbol{s}\|. \end{aligned} \tag{42}$$

Correspondingly, the derivative of $V_{\hat{f}} = \frac{1}{2}\hat{\boldsymbol{s}}^T\hat{\boldsymbol{s}}$ could be deduced as follows:

$$\begin{aligned}\dot{V}_{\hat{f}} =&\hat{\boldsymbol{s}}^T\dot{\hat{\boldsymbol{s}}} = \hat{\boldsymbol{s}}^T\widehat{\boldsymbol{W}}_1^T\boldsymbol{G}\left(\hat{\boldsymbol{X}}_1\right) \le G_{1M}\left\|\widehat{\boldsymbol{W}}_1\right\|\|\boldsymbol{s}-\boldsymbol{e}\|\\ \le&G_{1M}\left(W_{1M} + \left\|\widetilde{\boldsymbol{W}}_1\right\|\right)[(\alpha+1)\|\boldsymbol{s}\| + \gamma]. \end{aligned} \tag{43}$$

In view of (28), (42), (43), the time derivative of (41) could be derived as follows:

$$\dot{V} = \dot{V}_f + \dot{V}_{\hat{f}} + \dot{V}_{\widetilde{W}_1} + \dot{V}_{\widetilde{W}_2} \le F_1\|\boldsymbol{s}\|^2 + F_2\|\boldsymbol{s}\| + F_3, \tag{44}$$

where

$$\begin{cases} F_1 = (\alpha-1)k_2 + \alpha l_2\left(W_{2M} + \left\|\widetilde{\boldsymbol{W}}_2\right\|\right),\\ F_2 = G_{1M}(\alpha+1)\left(W_{1M} + \left\|\widetilde{\boldsymbol{W}}_1\right\|\right) + G_{2M}\left\|\widetilde{\boldsymbol{W}}_2\right\|\\ \qquad +\gamma l_2\left(W_{2M} + \left\|\widetilde{\boldsymbol{W}}_2\right\|\right) + \gamma k_2 + \varepsilon_2 + \|\boldsymbol{d}_{\max}\|,\\ F_3 = G_{1M}\left(W_{1M} + \left\|\widetilde{\boldsymbol{W}}_1\right\|\right)\gamma. \end{cases} \tag{45}$$

While $F_1$ could be divided as follows:

$$F_1 = -(1-q)k_2 - (qk_2 - F_{11}), \tag{46}$$

where $q \in (0,1)$ and $F_{11} = \alpha k_2 + \alpha l_2\left(W_{2M} + \left\|\widetilde{W}_2\right\|\right)$, since $k_2$ is a positive design parameter, $qk_2$ and $(1-q)k_2$ could be high enough as long as a high $k_2$ is selected. Therefore, in view of (39), the time derivative of (41) could be rewritten as follows:

$$\begin{aligned}\dot{V} =& -(1-q)k_2\|\boldsymbol{s}\|^2 - (qk_2 - F_{11})\|\boldsymbol{s}\|^2 + F_2\|\boldsymbol{s}\|\\ &+F_3 = -(qk_2 - F_{11})\left[\|\boldsymbol{s}\| - \frac{F_2}{2(qk_2 - F_{11})}\right]^2\\ &-(1-q)k_2\|\boldsymbol{s}\|^2 + \frac{F_2^2}{4(qk_2 - F_{11})} + F_3\\ \le& -(1-q)k_2\|\boldsymbol{s}\|^2 + \frac{F_2^2}{4(qk_2 - F_{11})} + F_3. \end{aligned} \tag{47}$$

Since $q \in (0,1)$, $k_2$, $\gamma$, $G_{1M}$, $W_{1M}$, $\sigma_1$, $\beta_1$ are positive constants, $\dot{V} \le 0$ could be guaranteed as long as $\|\boldsymbol{s}\|$ meet with following inequation:

$$\|\boldsymbol{s}\| \ge \sqrt{\frac{F_2^2 + 4(qk_2 - F_{11})F_3}{4k_2(1-q)(qk_2 - F_{11})}}. \tag{48}$$

Therefore, the variables $\boldsymbol{s}$ is upper bounded on the duration of flow, while the ultimate bound of $\|\boldsymbol{s}\|$ is

$$\|\boldsymbol{s}\| \le \sqrt{\frac{F_2^2 + 4(qk_2 - F_{11})F_3}{4k_2(1-q)(qk_2 - F_{11})}}. \tag{49}$$

Besides, the ultimate bound of $\|\hat{\boldsymbol{s}}\|$ is derived as follows:

$$\begin{aligned}\|\hat{\boldsymbol{s}}\| \le&\|\boldsymbol{s}\| + \|\boldsymbol{e}\| \le (\alpha+1)\|\boldsymbol{s}\| + \gamma\\ \le&(\alpha+1)\sqrt{\frac{F_2^2 + 4(qk_2 - F_{11})F_3}{4k_2(1-q)(qk_2 - F_{11})}} + \gamma. \end{aligned} \tag{50}$$

The ultimate bound of $\|\hat{\boldsymbol{s}}\|$ is acquired from (50). On the basis of all mentioned above, the following demonstration will illustrate the boundedness of all the variable signals in this proposed model-based control system during the jump instants.

**Circumstance 2 Jump instants** ($t = t_k$, $k = 1, 2, \ldots$)**:** Consider following candidate of Lyapunov function for the case at the jump instants

$$V = V_J + V_{\hat{f}} + V_{\widetilde{W}_1} + V_{\widetilde{W}_2}, \tag{51}$$

where $V_J = \frac{1}{2}\boldsymbol{s}^T\boldsymbol{s}$, $V_{\hat{f}} = \frac{1}{2}\hat{\boldsymbol{s}}^T\hat{\boldsymbol{s}}$, and $V_{\widetilde{W}_1}$, $V_{\widetilde{W}_2}$ are defined in Theorem 1. Substituting (22) into $V_J = \frac{1}{2}\boldsymbol{s}^T\boldsymbol{s}$ yields its first difference

$$\Delta V_J = \frac{1}{2}\left\|\boldsymbol{s}^+\right\|^2 - \frac{1}{2}\|\boldsymbol{s}\|^2 = 0, \;\; t = t_k. \tag{52}$$

Since $\hat{\boldsymbol{s}}^+ = \boldsymbol{s}$, the first difference of $V_f$ follows

$$\Delta V_{\hat{f}} = \frac{1}{2}\left\|\hat{\boldsymbol{s}}^+\right\|^2 - \frac{1}{2}\|\hat{\boldsymbol{s}}\|^2 \le -\frac{1}{2}\|\hat{\boldsymbol{s}}\|^2 + D, \;\; t = t_k, \tag{53}$$

where $D$ is the upper bound for the sliding vector $\boldsymbol{s}$ during the period of flow. Besides, for $\widetilde{\boldsymbol{W}}_1$ and $\widetilde{\boldsymbol{W}}_2$, (37) could be duplicated as follows:

$$\begin{aligned}\Delta V_{\widetilde{W}_1} + \Delta V_{\widetilde{W}_2} \le& -\frac{p_{11}}{2}\left\|\widetilde{\boldsymbol{W}}_1\right\|^2 - \frac{p_{12}}{2}\left\|\widetilde{\boldsymbol{W}}_2\right\|^2 + \bar{\zeta}_1\\ &+\bar{\zeta}_2 - \frac{p_{11}}{2}\left(\left\|\widetilde{\boldsymbol{W}}_1\right\| - \frac{p_{21}}{p_{11}}\right)^2\\ &-\frac{p_{12}}{2}\left(\left\|\widetilde{\boldsymbol{W}}_2\right\| - \frac{p_{22}}{p_{12}}\right)^2, \end{aligned} \tag{54}$$

where

$$\begin{cases} p_{11} = 2\sigma_1(1-\sigma_1), p_{12} = 2\sigma_2(1-\sigma_2),\\ p_{21} = 2[\beta_1\lambda_1 G_{M1}(1-\sigma_1) + \sigma_1 W_{M1}],\\ p_{22} = 2[\beta_2\lambda_2 G_{M2}(1-\sigma_2) + \sigma_2 W_{M2}],\\ \zeta_1 = 2\beta_1\sigma_1\lambda_1 G_{M1}W_{M1} + 2\sigma_1^2 W_{M1}^2 + \beta_1^2 G_{M1}^2\lambda_1^2,\\ \zeta_2 = 2\beta_2\sigma_2\lambda_2 G_{M2}W_{M2} + 2\sigma_2^2 W_{M2}^2 + \beta_2^2 G_{M2}^2\lambda_2^2,\\ \bar{\zeta}_1 = \zeta_1 + p_{21}^2/2p_{11}, \;\; \bar{\zeta}_2 = \zeta_2 + p_{22}^2/2p_{12}. \end{cases} \tag{55}$$

Substituting (52-55) into (51) lead to

$$\begin{aligned}\Delta V =&\Delta V_J+\Delta V_{\hat{f}}+\Delta V_{\widetilde{W}_1}+\Delta V_{\widetilde{W}_2}\\ \leq&-\frac{1}{2}\|\hat{\boldsymbol{s}}\|^2-\frac{1}{2}p_{11}\left\|\widetilde{\boldsymbol{W}}_1\right\|^2-\frac{1}{2}p_{12}\left\|\widetilde{\boldsymbol{W}}_2\right\|^2\\ &+\overline{\zeta}_1+\overline{\zeta}_2+D.\end{aligned}\tag{56}$$

Since $\overline{\zeta}_1$ and $\overline{\zeta}_2$ are positive constants according to (55), as long as following inequation is guaranteed

$$\|\hat{\boldsymbol{s}}\|>\sqrt{2\left(\overline{\zeta}_1+\overline{\zeta}_2+D\right)}.\tag{57}$$

Or following inequations are guaranteed

$$\begin{cases}\left\|\widetilde{\boldsymbol{W}}_1\right\|>\sqrt{2\left(\overline{\zeta}_1+\overline{\zeta}_2+D\right)/p_{11}},\\ \left\|\widetilde{\boldsymbol{W}}_2\right\|>\sqrt{2\left(\overline{\zeta}_1+\overline{\zeta}_2+D\right)/p_{12}}.\end{cases}\tag{58}$$

Then it's spontaneous to achieve a conclusion that $\Delta V<0$, at the trigger instants. Therefore, the boundedness of $\|\boldsymbol{s}\|$ and $\|\hat{\boldsymbol{s}}\|$ is guaranteed during both the flowing period and the trigger instants. According to theorem 2 proposed in [30], the global ultimate boundedness of $\|\boldsymbol{q}_{v,e}\|$, $\|\boldsymbol{\omega}_e\|$, $\|\boldsymbol{q}_{v,e}\|$, $\|\widehat{\boldsymbol{\omega}}_e\|$, $\|\boldsymbol{e}_1\|$, $\|\boldsymbol{e}_2\|$, $\|\boldsymbol{e}\|$ can be proved if the global ultimate boundedness of $\|\boldsymbol{s}\|$ and $\|\hat{\boldsymbol{s}}\|$ is proved. In addition, since $\widetilde{\boldsymbol{W}}_1$ and $\widetilde{\boldsymbol{W}}_2$ keep constant during the flow, and their boundedness are shown by Theorem 1, it's sure that all the system states are bounded whenever it is on the period of flowing or at the trigger instants. Hence, the conclusion that the model-based spacecraft dynamics model is global ultimately upper bounded (GUUB) has been demonstrated by means of these 2 theorems. □

### 4.3. Zeno behavior analysis

Since the boundedness of the impulsive dynamics system has been verified, only the Zeno behavior [42], which denotes the accumulation of consecutive triggering instants, may invalidate the control scheme. However, Zeno behavior could be avoided by appropriate control scheme design, the sequence of triggering could be continued as long as the IET is a positive number all the time. There is a radical variation in this paper that if the ETM is applied in the field of spacecraft attitude tracking control, it is not compulsory to ensure that the control orders must be executed discretely. In contrast with the compelling requirements proposed in [34], the wireless communication from the sensors to the controller is aperiodic, while the wireless communication from the controller to the actuators is periodic, thus, the communication pressure is eased and the attitude tracking precision could be guaranteed. Considering that the stability of the system has been proved by Theorem 1 and Theorem 2, the feasibility of this control method could be guaranteed by proving the impossibility of the Zeno Behavior.

**Theorem 3:** Take the attitude tracking dynamics model (1)-(3), inequation (5), the estimation model (15), the control law (19), the event-trigger error (20), the event-trigger condition (21) into consideration, it could be derived that there exists the lowest IET

$$T_k=t_{k+1}-t_k\geq\ln\left[1+\frac{\alpha\|\boldsymbol{q}_{v,e}(t_{k+1})\|+\gamma}{\|\boldsymbol{s}\|}\right]>0.\tag{59}$$

**Proof:** From (18), the following inequality holds for flowing period

$$\frac{d}{dt}\|\boldsymbol{e}\|=\frac{d}{dt}\sqrt{\boldsymbol{e}^T\boldsymbol{e}}=\frac{\boldsymbol{e}^T\dot{\boldsymbol{e}}}{\|\boldsymbol{e}\|}\leq\|\dot{\boldsymbol{e}}\|.\tag{60}$$

In view of Property 1, Assumption 4 and inequation (40), there is

$$\begin{aligned}\|\dot{\boldsymbol{e}}\|=&\|\dot{\boldsymbol{s}}-\dot{\hat{\boldsymbol{s}}}\|=\left\|\boldsymbol{J}^{-1}(\boldsymbol{L}+\boldsymbol{u}+\boldsymbol{d})-\widehat{\boldsymbol{W}}_1^T\boldsymbol{G}\left(\hat{\boldsymbol{X}}_1\right)\right\|\\ \leq&\left\|\tilde{\boldsymbol{L}}-k_2\boldsymbol{s}+k_2\boldsymbol{e}+\boldsymbol{d}\right\|/\boldsymbol{J}_{\min}+\left\|\widehat{\boldsymbol{W}}_1^T\boldsymbol{G}\left(\hat{\boldsymbol{X}}_1\right)\right\|\\ \leq&\left(\|\tilde{\boldsymbol{L}}\|+k_2\|\boldsymbol{s}\|+k_2\|\boldsymbol{e}\|+\|\boldsymbol{d}_{\max}\|\right)/\boldsymbol{J}_{\min}\\ &+\left\|\widehat{\boldsymbol{W}}_1^T\boldsymbol{G}(\boldsymbol{X}_1)-\widehat{\boldsymbol{W}}_1^T\left[\boldsymbol{G}(\boldsymbol{X}_1)-\boldsymbol{G}\left(\hat{\boldsymbol{X}}_1\right)\right]\right\|\\ \leq&\left[\left\|\widetilde{\boldsymbol{W}}_2\right\|G_{2M}+l_2\left(W_{2M}+\left\|\widetilde{\boldsymbol{W}}_2\right\|\right)\|\boldsymbol{e}\|+\varepsilon_2\right]/\boldsymbol{J}_{\min}\\ &+\left(k_2\|\boldsymbol{s}\|+k_2\|\boldsymbol{e}\|+\|\boldsymbol{d}_{\max}\|\right)/\boldsymbol{J}_{\min}\\ &+\left(W_{1M}+\left\|\widetilde{\boldsymbol{W}}_1\right\|\right)G_{1M}+l_1\left(W_{1M}+\left\|\widetilde{\boldsymbol{W}}_1\right\|\right)\|\boldsymbol{e}\|.\end{aligned}\tag{61}$$

Since the ultimate boundedness of $\|\boldsymbol{s}\|$, $\left\|\widetilde{\boldsymbol{W}}_1\right\|$, $\left\|\widetilde{\boldsymbol{W}}_2\right\|$ has been substantiated, substitute (60) to (61) leads to

$$\frac{d}{dt}\|\boldsymbol{e}\|\leq\mathrm{A}\|\boldsymbol{e}\|+B,\tag{62}$$

where $A=l_1(W_{1M}+\|\widetilde{\boldsymbol{W}}_1\|)+[l_2(W_{2M}+\|\widetilde{\boldsymbol{W}}_2\|+k_2)]/\boldsymbol{J}_{\min}$, $B=(G_{2M}\|\widetilde{\boldsymbol{W}}_2\|+k_2\|\boldsymbol{s}\|+\|\boldsymbol{d}_{\max}\|+\varepsilon_2)/\boldsymbol{J}_{\min}+G_{1M}W_{1M}+G_{2M}\|\widetilde{\boldsymbol{W}}_2\|$, Considering that $\|\boldsymbol{e}\|_{t=t_k}=0$ at the triggering instants, solving the differential inequation (62) leads to

$$\|\boldsymbol{e}\|\leq\frac{B}{A}\exp\left[A\left(t-t_k\right)-1\right].\tag{63}$$

Since $\|\boldsymbol{e}\|$ will be reset as zero at the event-triggering instants owing to the reset of the estimation model, there exists $\|\boldsymbol{e}\left(t_{k+1}\right)\|=\alpha\|\boldsymbol{s}\left(t_{k+1}\right)\|+\gamma$ at the triggering instants, consequently, substituting this instantaneous equation into (63) will lead to

$$\alpha\|\boldsymbol{s}\left(t_{k+1}\right)\|+\gamma\leq\frac{B}{A}\exp\left[A\left(t_{k+1}-t_k\right)-1\right].\tag{64}$$

Therefore, the IET owns its lower bound as follows:

$$T_i=t_{k+1}-t_k\geq\frac{\ln\left[\frac{A}{B}\left(\alpha\|\boldsymbol{s}\left(t_{k+1}\right)\|+\gamma\right)\right]+1}{A}.\tag{65}$$

Since all the components of $A$ and $B$ are positive constants or upper bounded by positive constants, $\alpha$ and $\gamma$ are design parameters, $\boldsymbol{s}(t_{k+1})$ is upper bounded with (41). Hence, it could be substantiated that $T_k > 0$ all the time. In other words, the Zeno Behavior is avoided. □

**Remark 4:** $\alpha$ and $\gamma$ are 2 positive constants very close to zero. According to (49), smaller $\alpha$ and smaller $\gamma$ will improve the accuracy of the system. However, according to (65), it will also prolong the IET and the burden over the communication channels will be aggravated. Thus, it's reasonable to balance the control precision and the communication pressure when tuning $\alpha$ and $\gamma$ according to (49) and (65).

**Remark 5:** In the ETC attitude control schemes, the attitude information is transmitted from the sensor module to the control module. During the event-triggered interval, there is no attitude information to be transmitted, and the zero-order holds [34] are used to hold the last transmitted attitude information in the existing ETC attitude control schemes. However, the event-triggered errors between the last transmitted attitude and the actual attitude will substantially affect the attitude control precision [34, 35]. In order to suppress the effect of the event-triggered errors on attitude control performance, a NN estimation model is employed to replace the zero-order holds in the proposed control scheme. The NN estimation model is proposed to estimate the attitude of spacecraft during the event-triggered intervals based on the last transmitted attitude information. As a result, the proposed ETM is more difficult to be violated compared with the zero-order holds based ETM. Because $\|\boldsymbol{e}\| = \|\boldsymbol{s} - \hat{\boldsymbol{s}}\|$ resulted from the proposed control system is varying slower than $\|\boldsymbol{e}\| = \|\boldsymbol{s} - \boldsymbol{s}(t_i)\|$ resulted from the corresponding static event-triggered attitude control system since $\hat{\boldsymbol{s}}$ is varying to approximate $\boldsymbol{s}$ while $\boldsymbol{s}(t_i)$ keeps stable during the flow period. Therefore, the model-based ETM can lead to higher control precision with the same triggering frequency.

**Remark 6:** In this paper, the proposed control system is global ultimately upper bounded, which means for any compact set, there exists a controller with sufficient NN nodes to ensure all the signals in the resulting closed-loop system are bounded when the initial states are within the set. To avoid too much computation, the amount of the NN nodes is limited in numerical simulation. Therefore, the approximation ability of the NN system is limited and it's necessary to set some constraints on the compact set to guarantee the effectiveness of such an approximation. More details can be seen in [27] and [43].

## 5. SIMULATION STUDIES

In this section, simulation instances are displayed to verify the proposed model-based attitude tracking ETC system for spacecraft with limited communication. Since the disabled spacecraft with enough value to reactivate are always those huge ones, the spacecraft's inertia matrix $\boldsymbol{J}$ [5] [34] is assumed as

$$\boldsymbol{J} = \begin{bmatrix} 1148 & 60 & 65 \\ 60 & 1142 & 70 \\ 65 & 70 & 1141 \end{bmatrix} \text{ kg·m}^2. \tag{66}$$

From (66), even though the size of this spacecraft is large enough, since the output torque of the flywheels are limited, it's unavoidable to consider the problem of actuator saturation. Thus, it's reasonable to set the maximum of the wheel's output torque as 1 N·m for each axis. In addition, the initial angular velocity error, also the initial one of the estimation model is selected as $\boldsymbol{\omega}_{e0} = \widehat{\boldsymbol{\omega}}_{e0} = \begin{bmatrix} 0.6 & -0.6 & -0.6 \end{bmatrix}^T$ rad/s, besides, the initial attitude tracking errors of the two models are chosen as $\boldsymbol{q}_{v,e0} = \widehat{\boldsymbol{q}}_{v,e0} = [\sin(3^\circ) \quad \sin(4^\circ) \quad -\sin(2.5^\circ)]^T$, the aimed attitude quaternion is chosen as $\boldsymbol{q}_{d0} = \begin{bmatrix} 1 & 0 & 0 & 0 \end{bmatrix}^T$, besides, the time-varying desired angular velocity is supposed as $\boldsymbol{\omega}_d = 0.5 \times [\sin(\pi t/200) \quad \sin(\pi t/200) \quad \sin(\pi t/200)]^T$ deg/s, the external disturbances which are applied in this simulation are assumed as $\boldsymbol{d}(t) = [1 + 2\sin(0.5t) - 1 - 5\sin(0.5t) \quad 2 + 4\cos(0.5t)]^T \times 10^{-3}$ N·m. Besides, attitude measurement errors by the gyroscopes and the star-sensors, respectively, have been considered in this simulation, which is always ignored by almost all the previous theoretical research in the area of spacecraft attitude tracking control. The measurement error of the gyroscope is considered as 0.0002 deg/s, while the measurement errors of the star-sensors could be divided into system error and random error, the quantity of the system error is considered as 0.01 deg, besides, the quantity of the random error is considered as 0.002 deg.

The basis function of the neural network is selected as the Gaussian function which contains 11 hidden-layer nodes, and these nodes are evenly distributed in $[-0.5, 0.5]$ with their widths $H = 1$. The initial state of the neural network is a $11 \times 3$ matrix whose elements are all zero. The control parameters are chosen as $k_1 = 0.2$, $k_2 = 150$. The maximum control torques in roll channel, pitch channel and yaw channel are supposed to be 0.2 N·m. The event-trigger parameters are set as $\alpha = 0.01$, $\gamma = 1 \times 10^{-5}$. In addition, the parameters of the adaptive law (19) are selected to be $\sigma_1 = 0.00175$, $\sigma_2 = 0.0011$, $\beta_1 = \beta_2 = 0.01$, $c_1 = c_2 = 0.01$ for $\widehat{\boldsymbol{W}}_1$ and $\widehat{\boldsymbol{W}}_2$ respectively.

The attitude tracking error of the spacecraft is displayed in Fig. 2. Here, the attitude tracking errors are shown as Euler angles, which are derived from unit quaternion for interpreting the results clearly in the simulation. Besides, to demonstrate the high estimation precision of the estimation model, the difference between the real model and the estimation model in tracking errors is illustrated in Fig. 3. Similarly, Fig. 4 exhibits the angular velocity tracking errors of the spacecraft while Fig. 5 displays the difference between the two models in angular velocity tracking errors. Figs. 2-5 show that $\boldsymbol{q}_{v,e}$, $\widehat{\boldsymbol{q}}_{v,e}$, $\widetilde{\boldsymbol{q}}_{v,e}$, $\boldsymbol{\omega}_e$, $\widehat{\boldsymbol{\omega}}_e$, $\widetilde{\boldsymbol{\omega}}_e$ are all

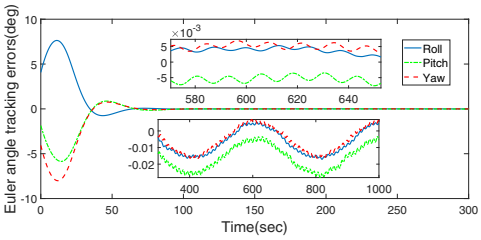


Fig. 2. Attitude tracking error.

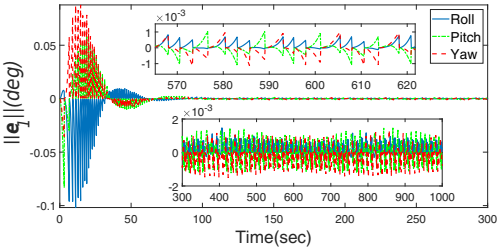


Fig. 3. Difference in attitude tracking error.

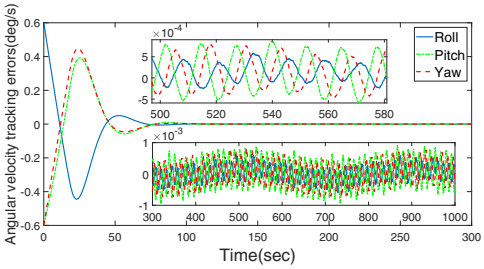


Fig. 4. Angular velocity tracking error.

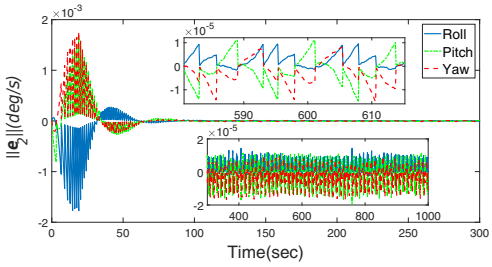


Fig. 5. Difference in angular velocity tracking error.

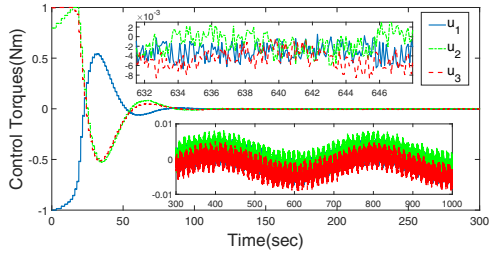


Fig. 6. Control Torques $\boldsymbol{u}(t)$.

ultimately bounded within acceptable ranges. The control torques are shown in Fig. 6. It's viewed that the control torques tend to a small bound.

The cumulative times of triggered-event are illustrated in Fig. 7, the number of the triggering instants within

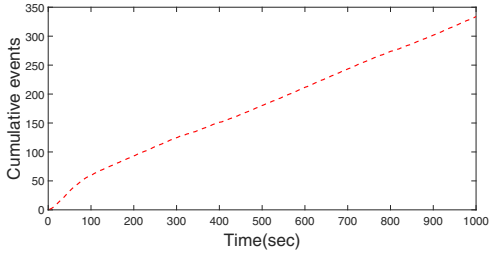


Fig. 7. Cumulative event numbers.

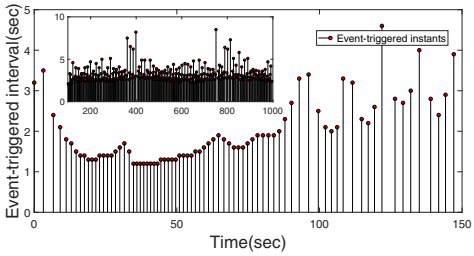


Fig. 8. The variation of the IET(Sec).

1000 seconds is 332, in other words, the triggered mechanism will be violated a time every 3.012 seconds on average. Considering a conventional time-triggered attitude tracking control system with an 8 Hz sampling frequency, the control information ought to be sent 8000 times over the wireless communication channel, while the simulation demonstrates that only 332 times of data transmission happens in 1000 seconds. Hence, the size of data communication is conspicuously decreased by 95.85% owing to the proposed control strategy. Correspondingly, Fig. 8 exhibits the variation of the IET between each two nearest events. It is observed that there exists the minimum IET, which is about 1.2 seconds in this simulation. Table 1 demonstrates the comparison among the proposed control scheme and other control schemes in minimum IET, mean IET, ATE (the maximum attitude tracking error appears on 3 axes under the state of stabilization) and AVTE (the maximum angular velocity tracking error appears on 3 axes under the state of stabilization).

In Table 1, scheme 1 denotes the proposed model-based ETC system designed in this paper for spacecraft attitude tracking, scheme 2 denotes a latest adaptive NN ETC scheme for attitude tracking [44], scheme 3 denotes a latest adaptive ETC scheme for attitude tracking with the ability to deal with unknown actuator faults [45], scheme 4 denotes the traditional high-precision attitude tracking control scheme adopted in current satellites with wireless network system to transmit signals in their control system. The control frequency of traditional high-precision attitude control is 4 Hz or more than 4 Hz, and the minimum IET is equal to the mean IET in scheme 4 as a result of uniform control sampling.

According to Table 1, scheme 1 proposed in this paper presents the longest mean IET and the longest min-

Table 1. Comparison among ETC systems for the attitude tracking of spacecraft.

| | Sch1 | Sch2 | Sch3 | Sch4 |
|---|---|---|---|---|
| Minimum IET(sec) | 1.2 | 0.1 | 0.05 | $\leq 0.25$ |
| Mean IET(sec) | 3.01 | 2.85 | 0.13 | $\leq 0.25$ |
| ATE (deg) | 0.03 | 0.06 | 3 | $\leq 0.05$ |
| AVTE (deg/s) | 0.001 | 0.001 | 0.03 | $\leq 0.001$ |

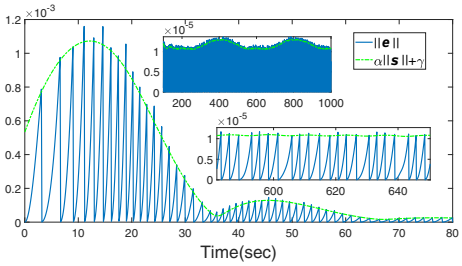


Fig. 9. The evolution of the event-triggering condition.

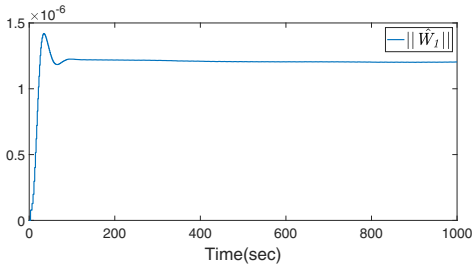


Fig. 10. The variation of $\left\|\widehat{\boldsymbol{W}}_1\right\|$.

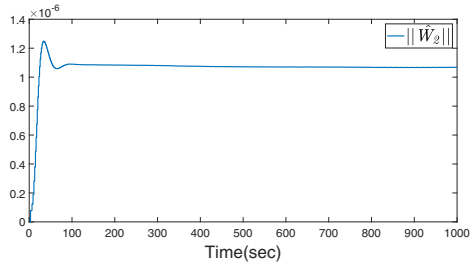


Fig. 11. The variation of $\left\|\widehat{\boldsymbol{W}}_2\right\|$.

imum IET compared with other event-triggered control schemes designed for spacecraft attitude tracking, which demonstrates the ETC system proposed in this paper is the best one in dealing with spacecraft attitude tracking control with limited communication. Besides, minimum IET is a character parameter always neglected in previous research, while too low minimum IET may put too much pressure on the communication channels in a short time. The low minimum IET shown by previous research may bring some risk to engineering practice, while the model-based ETC approach proposed in this paper avoids the potential risk. Fig. 9 shows the variation of the event-triggering condition. Fig. 10 and Fig. 11 show the norm variation of $\widehat{\boldsymbol{W}}_1$ and $\widehat{\boldsymbol{W}}_2$. It's obvious that the approximation state of the NN weight matrices is ultimately bounded complying with an aperiodic updating law. Thus, in accordance with the results of the simulation, all the signals are ultimately bounded in the proposed attitude tracking ETC system. The high precision shown by the numerical simulation results substantiate the strong robustness of the model-based ETC method. Besides, the proposed model-based ETC system demonstrates its ability to ease the pressure over the communication channel with a very high tracking precision compared with the latest relevant research [44, 45]. The proposed model-based ETC system also behaviors well in dealing with potential time delay. Consider that there is no obvious difference between the numerical simulation with time delay and that without time delay, the numerical simulation with time delay is not present in this paper. Obviously, the numerical simulation verify the theoretical findings and the effectiveness of the proposed scheme.

## 6. CONCLUSION

An adaptive ETC scheme with the aid of an estimation model is proposed for spacecraft attitude tracking with limited communication and external disturbances in this paper. In the proposed strategy, the estimation model takes the place of the ZOHs which are used in conventional event-triggered control. This estimation model is employed to match the dynamics model of the spacecraft and an ETM is employed to contrast the spacecraft dynamics model with the estimation model. Once the difference between the real model and the estimation model violates the event-triggering condition, the ETC mechanism will be triggered and the state of the estimation model will be reset as the state measured by the sensors fixed on the spacecraft instantly. The stability of the proposed control scheme is proved by the Lyapunov method under both the flow state and the jump state. Correspondingly, the results of simulation demonstrate the effectiveness of the proposed model-based control method, the attitude angular velocity error of the spacecraft could be stabilized within the bound of 0.001 deg/s, which is accurate enough for nearly all the known spacecraft missions, besides, the communication burden over the communication channel is less than 5 percent of that one without event-triggered strategy. Finally, the results of the simulation also verify the theoretical analysis.

## REFERENCES

[1] H. Tanaka, N. Yamamoto, T. Yairi, and K. Machida, "Reconfigurable cellular satellites maintained by space robots," *Journal of Robotics and Mechatronics*, vol. 18, no. 3, pp. 356-364, 2006.

[2] D. Barnhart, B. Sullivan, and R. Hunter, "Phoenix program status-2013," *Proc. of AIAA SPACE Conference and Exposition*, 2013.

[3] J. Weise, K. Brieß, A. Andreé, H. G. Reimerdes, and M. Göller, "An intelligent building blocks concept for on-orbit-satellite servicing," *Proceedings of the International Symposium on Artificial Intelligence, Robotics and Automation in Space (iSAIRAS)*, 2012.

[4] H. Chang, P. Huang, and Y. Zhang, "Distributed control allocation for spacecraft attitude takeover control via cellular space robot," *Journal of Guidance, Control, and Dynamics*, vol. 41, no. 11, pp. 2499-2506, 2018.

[5] H. Chang, P. Huang, and Y. Zhang, "Cellular space robot and its interactive model identification for spacecraft takeover control," *Proc. of IEEE/RSJ International Conference on Intelligent Robots and Systems(IROS)*, IEEE, 2016.

[6] W. Xu, D. Meng, and Y. Chen, "Dynamics modelling and analysis of a flexible-base space robot for capturing large flexible spacecraft," *Multibody System Dynamics*, vol. 32, no. 3, pp. 357-401, 2014.

[7] M. Shan, J. Guo, and E. Gill, "Review and comparison of active space debris capturing and removal methods," *Progress in Aerospace Sciences*, vol. 80, pp. 18-32, Jan. 2007.

[8] J. Ahmed, V. T. Coppola, and D. S. Bernstein, "Adaptive asymptotic tracking of spacecraft attitude motion with inertia matrix identification," *Journal of Guidance, Control, and Dynamics*, vol. 21, no. 5, pp. 684-691, 1998.

[9] G. Wu, S. Song, and J. Sun, "Adaptive dynamic surface control for spacecraft terminal safe approach with input saturation based on tracking differentiator," *International Journal of Control, Automation and Systems*, vol. 16, no. 3, pp. 1129-1141, 2018.

[10] W. Luo, Y. Chu, and K. Ling, "Inverse optimal adaptive control for attitude tracking of spacecraft," *IEEE Transactions on Automatic Control*, vol. 50, no. 11, pp. 1639-1654, 2005.

[11] F. Bayat, "Model predictive sliding control for finite-time three-axis spacecraft attitude tracking," *IEEE Transactions on Industrial Electronics*, vol. 66, no. 10, pp. 7986-7996, 2019.

[12] J. D. Boskovic, S.-M. Li, and R. K. Mehra, "Robust adaptive variable structure control of spacecraft under control input saturation," *Journal of Guidance, Control, and Dynamics*, vol. 24, no. 1, pp. 14-22, 2001.

[13] Q. Hu, B. Xiao, D. Wang, and E. K. Poh, "Attitude control of spacecraft with actuator uncertainty," *Journal of Guidance, Control, and Dynamics*, vol. 36, no. 6, pp. 1771-1776, 2013.

[14] P. Chutiphon, "Output feedback second order sliding mode control for spacecraft attitude and translation motion," *International Journal of Control, Automation and Systems*, vol. 14, no. 2, pp. 411-424, 2016.

[15] B. Wu, D. Wang, and E. K. Poh, "High precision satellite attitude tracking control via iterative learning control," *Journal of Guidance, Control, and Dynamics*, vol. 38, no. 3, pp. 528-534, 2014.

[16] G. N. Nair, D. Wang, and E. K. Poh, "Feedback control under data rate constraints: an overview," *Proceedings of the IEEE*, vol. 95, no. 1, pp. 108-137, 2007.

[17] S. Tatikonda and S. Mitter, "Control under communication constraints," *IEEE transactions on Automatic Control*, vol. 49, no. 7, pp. 1056-1068, 2004.

[18] J. Zhou, C. Wen, and G. Yang, "Adaptive backstepping stabilization of nonlinear uncertain systems with quantized input signal," *IEEE Transactions on Automatic Control*, vol. 59, no. 2, pp. 460-464, 2014.

[19] J. Xie, Y. Kao, C. Zhang, and H. R. Karimi, "Quantized control for uncertain singular Markovian jump linear systems with general incomplete transition rates," *International Journal of Control, Automation and Systems*, vol. 15, no. 3, pp. 1107-1116, 2017.

[20] H. Ma, Q. Zhou, L. Bai, and H. Liang, "Observer-based adaptive fuzzy fault-tolerant control for stochastic nonstrict-feedback nonlinear systems with input quantization," *IEEE Transactions on Systems, Man, and Cybernetics: Systems*, vol. 49, no. 2, pp. 287-298, 2019.

[21] P. Tabuada, "Event-triggered real-time scheduling of stabilizing control tasks," *IEEE Transactions on Automatic Control*, vol. 52, no. 9, pp. 1680-1685, 2007.

[22] J. Lunze and D. Lehmann, "A state-feedback approach to event-based control," *Automatica*, vol. 46, no. 1, pp. 211-215, 2010.

[23] P. Huang, F. Zhang, J. Cai, D. Wang, Z. Meng, and J. Guo, "Dexterous tethered space robot design, measurement, control and experiment," *IEEE Transactions on Aerospace and Electronic Systems*, vol. 53, no. 3, pp. 1452-1468, 2017.

[24] J. Liu, J. Fang, Z. Li, and G. He, "Formation control with multiple leaders via event-triggering transmission strategy," *International Journal of Control, Automation and Systems*, vol. 17, no. 6, pp. 1494-1506, 2019.

[25] Z. Tang and C. Li, "Distributed event-triggered containment control for discrete-time multi-agent systems," *International Journal of Control, Automation and Systems*, vol. 16, no. 6, pp. 2727-2732, 2018.

[26] A. Sahoo, H. Xu, and S. Jagannathan, "Event-based neural network approxmation and control of uncertain nonlinear continuous-time systems," *Proc. of American Control Conference*, pp. 1567-1572, 2015.

[27] Y. Li and G. Yang, "Model-based adaptive event-triggered control of strict-feedback nonlinear systems," *IEEE Transactions on Neural Networks and Learning Systems*, vol. 29, no. 4, pp. 1033-1045, 2018.

[28] Y. Li and G. Yang, "Adaptive neural control of pure-feedback nonlinear systems with event-triggered communications," *IEEE Transactions on Neural Networks and Learning Systems*, vol. 29, no. 12, pp. 6242-6251, 2018.

[29] X. Li, D. Ma, X. Hu, and Q. Sun, "Dynamic event-triggered control for heterogeneous leader-following consensus of multi-agent systems based on input-to-state stability," *International Journal of Control, Automation and Systems*, vol. 18, no. 2, pp. 293-302, 2020.

[30] B. Wu, "Spacecraft attitude control with input quantization," *Journal of Guidance, Control, and Dynamics*, vol. 39, no. 1, pp. 176-181, 2015.

[31] B. Wu and X. Cao, "Roubust attitude tracking control for spacecraft with quantized torques," *IEEE transactions on Aerospace and Electronic Systems*, vol. 54, no. 2, pp. 1020-1028, 2018.

[32] H. Sun, L. Hou, G. Zong, and X Yu, "Fixed-time attitude tracking control for spacecraft with input quantization," *IEEE Transactions on Aerospace and Electronic systems*, vol. 55, no. 1, pp. 124-134, 2019.

[33] C. Zhang, J. Wang, D. Zhang, and X. Shao, "Learning observer based and event-triggered control to spacecraft against actuator faults," *Aerospace Science and Technology*, vol. 78, no. 7, pp. 522-530, 2018.

[34] B. Wu, Q. Shen, and X. Cao, "Event-triggered attitude control of spacecraft," *Advances in Space Research*, vol. 61, no. 3, pp. 927-934, 2018.

[35] L. Xing, C. Wen, Z. Liu, H. Su, and J. Cai, "An event-triggered design scheme for spacecraft attitude control," *Pro.co f 12th IEEE Conference on Industrial Electronics and Applications*, 2017.

[36] M. Lovera and A. Astolfi, "Spacecraft attitude control using magnetic actuators," *Automatica*, vol. 40, no. 8, pp. 1405-1414, 2004.

[37] M. H. Stone, "The generalized Weierstrass approximation theorem," *Mathematics Magazine*, vol. 21, no. 5, pp. 237-254, 1948.

[38] F. W. Lewis, S. Jagannathan, and A. Yesildirak, *Neural Network Control of Robot Manipulators and Non-linear Systems*, CRC press, 1998.

[39] L. Wang, "Stable adaptive fuzzy control of nonlinear systems," *IEEE Transactions on Fuzzy Systems*, vol. 1, no. 2, pp. 146-155, 1993.

[40] J. Sarangapani, *Neural Network Control of Nonlinear Discrete-time Systems*, CRC press, 2006.

[41] S. Ge, C. Yang, S. Dai, Z. Jiao, and T. Lee, "Robust adaptive control of a class of nonlinear strict-feedback discrete-time systems with exact output tracking," *Automatica*, vol. 45, no. 11, pp. 2537-2545, 2009.

[42] R. Postoyan, P. Tabuada, D. Nesic, and A. Anta, "A framework for the event-triggered stabilization of nonlinear systems," *IEEE Transactions on Automatic Control*, vol. 60, no. 4, pp. 982-996, 2015.

[43] S. Ge, C. Yang, and T. Lee, "Adaptive predictive control using neural network for a class of pure-feedback systems in discrete time," *IEEE Transactions on Neural Networks*, vol. 19, no. 9, pp. 15991614, Sep. 2008.

[44] W. Liu, Y. Geng, B. Wu, and D. Wang, "Neural-network-based adaptive event-triggered control for spacecraft attitude tracking," *IEEE Transactions on Neural Networks and Learning Systems*, 2019. DOI: 10.1109/TNNLS.2019.2951732

[45] C. Wang, L. Guo, C. Wen, Q. Hu and J. Qiao, "Event-triggered adaptive attitude tracking control for spacecraft with unknown actuator faults," *IEEE Transactions on Industrial Electronics*, vol. 67, no. 3, pp. 2241-2250, 2020.

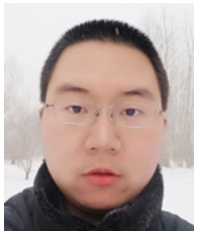

**Hongyi Xie** received his B.Eng. degree in 2018 in the major of flight vehicle design and engineering from the Harbin Institute of Technology, Harbin, China, where he is currently pursuing a degree of master with the Research Center of Satellite Technology. His research interests are spacecraft attitude control and on-orbit services.

**Baolin Wu** received his B.Eng. and M.Eng. degrees in spacecraft design from the Harbin Institute of Technology, Harbin, China, in 2003 and 2005, respectively, and a Ph.D. degree in spacecraft formation control from Nanyang Technological University, Singapore, in 2011. From 2011 to 2013, he spent two years in the satellite research and development industry in ST Electronics (Satellite Systems) Pte Ltd., Singapore. He developed algorithms for satellite attitude determination and control system. He joined in Research Center of Satellite Technology, Harbin Institute of Technology in 2014. He is currently a full professor. His current research area is in spacecraft attitude control, attitude synchronization, spacecraft formation control, and trajectory optimization.

**Weixing Liu** received his B.Eng. and M.Eng. degrees in spacecraft design from the Harbin Institute of Technology, Harbin, China, in 2015 and 2017, respectively, where he is currently pursuing a Ph.D. degree with the Research Center of Satellite Technology. His research interests are spacecraft attitude control and on-orbit services.